Structural and electronic properties of carbon in hybrid diamond-graphite structures

Filipe J. Ribeiro,[1] Paul Tangney,[2] Steven G. Louie,[1] and Marvin L. Cohen[1]
[1]*Department of Physics, University of California, Berkeley, California 94720-0001, USA and Material Sciences Division, Lawrence Berkeley National Laboratory, Berkeley, California 94720-0001, USA*
[2]*The Molecular Foundry, Lawrence Berkeley National Laboratory, Berkeley, California 94720-0001, USA*
(Received 6 March 2005; revised manuscript received 13 October 2005; published 7 December 2005)

In this paper we report on *ab initio* pseudopotential density-functional calculations of some possible high-pressure phases of carbon. The total energies of several hybrid diamond-graphite structures were calculated as a function of volume using density-functional theory and the local density approximation. The lowest calculated transition pressures between hexagonal-graphite and hybrid structures were 17 and 20 GPa, which compare well with the experimental value of 14 GPa for the transition at low temperatures between graphite and a still unidentified hard transparent phase. The electronic densities of states for the different structures are presented. Also, the x-ray powder diffraction patterns for a few structures were simulated and qualitatively compared to published experimental diffraction patterns.

DOI: 10.1103/PhysRevB.72.214109 PACS number(s): 71.15.Mb, 61.66.Bi, 64.70.Dv, 62.50.+p

I. INTRODUCTION

At ambient conditions of pressure and temperature, the most stable crystalline structure of carbon is hexagonal-graphite.[1] Without the use of catalysts, graphite can be converted to diamond at pressures above 15 GPa and high temperatures (>1000 °C).[1–4] Molecular dynamics studies[5] have shown that the graphite layers shift relative to one another under pressure and that for high enough temperatures, an abrupt buckling of the graphite sheets yields a mixture of both cubic and hexagonal symmetric diamond structures. The high temperatures required to induce the phase transition is indicative of a strong activation barrier between graphite and diamond.

On the other hand, if the temperature is kept low while applying pressure to graphite, a transition still occurs to a high-resistance, low-optical reflectivity transparent phase distinct from diamond for pressures above 14 GPa.[1,4,6–8] If pressure is released, carbon reverts back to the graphite structure unless the temperature is below 100 K.[7] This means that this transparent phase is metastable relative to graphite, and the low temperature is indicative of a very low activation barrier between the graphite and transparent phases. A remarkable property of this transparent phase is its exceptional hardness. This was revealed in recent experiments[8] by the broadening of ruby fluorescence lines and the ring crack indentation left on the diamond anvil after decompression. Other experiments on cold compression of carbon nanotubes have also found a quenchable superhard phase.[9] Although a great deal of work has been done to identify this transparent phase[1,4,6–8] and many structures have been proposed, details of the atomic structure remain elusive.

Here calculations of the electronic and structural properties of several possible carbon structures are discussed and compared to experimental results. Cubic-diamond and hexagonal-graphite have been studied earlier,[10–14] and some results are repeated here for comparison to new structures.

II. STRUCTURES

Diamond is present in nature in the cubic form, space group $Fd\bar{3}m$, where all the atoms are bound to each other with tetrahedral (sp^3) coordination. We will refer to this phase of diamond as cubic-diamond. In 1967, Bundy and Kasper[4] synthesized a form of diamond with hexagonal symmetry by applying pressures in excess of 13 GPa at 1000 °C to graphite. This hexagonal phase, also known as lonsdaleite, has the space-group symmetry of $P6_3/mmc$, and all the electron orbitals are sp^3 hybridized just as in cubic-diamond.

Graphite is composed of layers of carbon atoms stacked on top of each other where the electron orbitals are sp^2 hybridized. The most stable stacking of these carbon layers corresponds to the ABAB stacking shown in Fig. 1(a). We will refer to it as hexagonal-graphite. Because of the change in symmetry, the transition from graphite to either cubic or hexagonal-diamond requires that the graphite planes slide

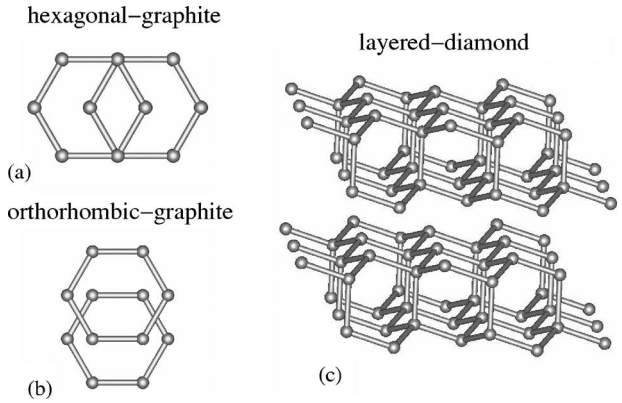

FIG. 1. Top views of (a) hexagonal-graphite, (b) orthorhombic-graphite, and (c) the layered-diamond structure obtained directly from hexagonal-graphite through buckling and without any graphene plane sliding.

 ©2005 The American Physical Society

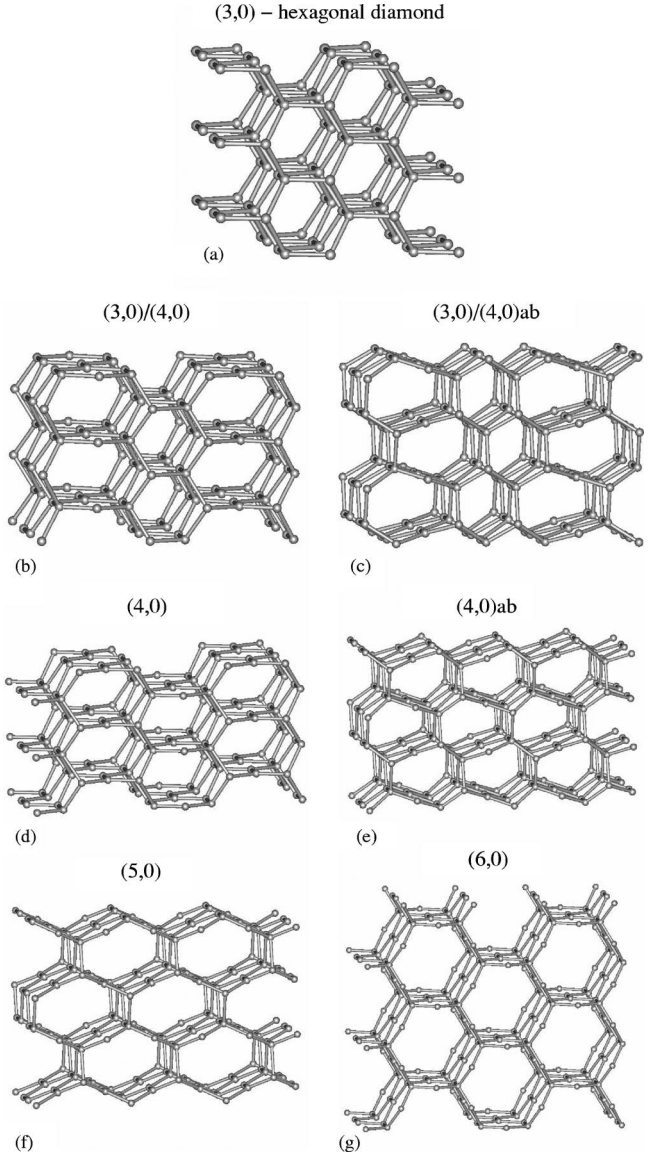

FIG. 2. The honeycomb structures: (a) all sp^3 (3,0) honeycomb structure (hexagonal-diamond), (b) mixed (3,0) and (4,0) structure, (c) mixed (3,0) and (4,0)ab structure, (d) (4,0) structure, (e) AB-stacked (4,0)ab structure, (f) (5,0) structure, and (g) (6,0) hexagonal structure. All except (6,0) can be obtained from buckling orthorhombic-graphite.

from their equilibrium positions.[5] This breaks the hexagonal symmetry and results in a structure referred to as orthorhombic-graphite [see Fig. 1(b)]. If no sliding is allowed, one could imagine that the layers of hexagonal-graphite could still buckle and form sp^3-sp^3 bonds in between graphite layers, giving rise to a layered diamondlike structure as shown in Fig. 1(c).

Figures 2(a)–2(g) show a class of structures composed of a mixture of sp^2-sp^2 and sp^3-sp^3 bonds. These structures, due to their symmetry, will be referred to as honeycomb structures. Each of the individual honeycombs can be viewed as a very narrow zigzag carbon nanotube, and an index of the form (m,n) can be associated with it (see, for example, Ref. 15 for a description of nanotube indexing). The (3,0) honeycomb is, in fact, the hexagonal-diamond structure, which, as discussed above, can be obtained by buckling orthorhombic-graphite. All the other honeycombs, except the (6,0), can also be obtained from buckling orthorhombic-graphite. The (6,0) honeycomb could potentially be synthesized by carbon deposition on a carefully engineered substrate. The $(3,0)/(4,0)$ and the $(3,0)/(4,0)$ab are hybrid structures, where half the honeycombs are (3,0) and the other half are (4,0) and (4,0)ab, respectively. These hybrids are obtained by buckling four out of five of the sp^2-bonded atoms in a graphite layer. The (4,0) honeycomb is characterized by a buckling of two out of three of every sp^2-bonded atom in each graphite layer, and depending on the particular stacking, different structures can be constructed, such as (4,0) and (4,0)ab. The (5,0) honeycomb can be obtained from the buckling of half of the sp^2-bonded atoms in graphite, whereas, as mentioned above, the (6,0) honeycomb cannot be obtained from buckling graphite layers. One important common factor of all the honeycomb structures is the pairing of sp^2 hybridized atoms, so that a π bond is established between the two, reinforcing the overall stability of the crystal.

Hybrid graphite-diamond structures similar to the ones studied here were suggested by Karfunkel and Dressler,[16] Balaban *et al.*,[17] and Umemoto *et al.*[18] Previous *ab initio* calculations for the strictly hexagonal (6,0), (9,0), and (12,0) honeycombs have been performed by Park and Ihm.[19]

There are many other possible structures and possible stackings of the different honeycombs studied here, including amorphous ones, but an exhaustive study is beyond the scope of this work.

III. COMPUTATIONAL DETAILS

For each crystal structure the total energy was calculated using density-functional theory.[20,21] The interaction between the valence electrons and the core electrons and nucleus of an atom was described by *ab initio* pseudopotentials.[22] Specifically, separable,[23] norm-conserving Troullier-Martins[24] pseudopotentials were used. The valence electron wave functions were expanded as linear combinations of plane waves with an energy cutoff of 70 Ry. The Brillouin zone was sampled on uniform k-point meshes.[25] The exchange and correlation energy was calculated using the local-density approximation to the energy functional.[26,27] The lattice parameters were all optimized at each pressure with a quasi-Newton method,[28] using the forces and stresses obtained through the Hellmann-Feynman theorem. From the calculated energies, the minimum of energy E_0, the equilibrium volume V_0, and the zero pressure bulk modulus B_0, were obtained from a fit to the empirical function

$$E(V) = E_0 + \frac{B_0}{V_0}\frac{(V-V_0)^2}{2} + E_1 F\left(\frac{V-V_0}{V_1}\right),$$

where E_1 and V_1 are two extra free parameters, and $F(x)$ is the function

$$F(x) = e^{-x} - \left(1 - x + \frac{x^2}{2}\right),$$

which, by construction, satisfies

$$F(x=0) = F'(x=0) = F''(x=0) = 0.$$

The electronic density of states was calculated using the tetrahedron method,[29] and the simulated x-ray powder diffraction patterns were obtained from the squares of the structure factors. Molecular-dynamics simulations based on the extended Tersoff-Brenner potential[30] and using a time step of 0.4 fs were performed on the equilibrium configurations of the proposed structures to investigate their dynamic stability.

IV. RESULTS

For all of the honeycombs, layered-diamond, hexagonal and orthorhombic-graphite, and cubic-diamond, Fig. 3(a) and 3(b) show the energy versus volume and enthalpy versus pressure curves, respectively, where the lines are numerical fits to the calculated points. In Fig. 3(b), the enthalpy lines of the (3,0)/(4,0), (3,0)/(4,0)ab, (4,0), (4,0)ab, and layered-diamond cross the enthalpy line of hexagonal-graphite at 17, 20, 34, 40, and 120 GPa, respectively. These intersections indicate the pressure at which one phase becomes thermodynamically more stable than the other at zero temperature.

Molecular-dynamics simulations of lengths of tens of picoseconds using supercells of dimension $5\times5\times5$ times the unit cell dimensions and at temperatures exceeding 1000 K at zero pressure suggest that all of the proposed structures—except layered-diamond and orthorhombic-graphite—are dynamically stable. This is not surprising given that all valence orbitals are essentially hybridized sp^2 or sp^3.

Layered-diamond is only metastable at high pressures. Attempts to relax the layered-diamond structure for pressures below 50 GPa resulted in a spontaneous phase transition to hexagonal-graphite, which is indicative of a very low or nonexistent activation barrier for the reverse transition. This instability could be related to the lack of a forth bond for half of the atoms on each buckled layer [see Fig. 1(c)]. Given that the activation energy for sliding of graphite planes is very small and the very high transition pressure between graphite and layered-diamond compared to all the other transition pressures, it is very unlikely that the layered-diamond phase can ever be observed experimentally.

Figure 3(c) shows the bulk modulus as a function of pressure for selected structures. The low-density honeycombs, such as (5,0) and (6,0), have a low bulk moduli (276 and 255 GPa at zero pressure, respectively) compared to the higher density ones (3,0)/(4,0), (3,0)/(4,0)ab, (4,0) and (4,0)ab, with bulk moduli of 397, 411, 356, and 361 GPa at zero pressure, respectively. When applying pressure to a solid, the reaction pressure from the solid depends on the strength of each atomic bond and on the number of bonds per unit volume. The more bonds per unit volume a solid has, the lower its compressibility, which explains the increase in bulk modulus with density in the honeycombs. It is noteworthy that, within our model fit, (3,0)/(4,0) is expected to be less compressible than diamond for pressures above 120 GPa [see Fig. 3(c)].

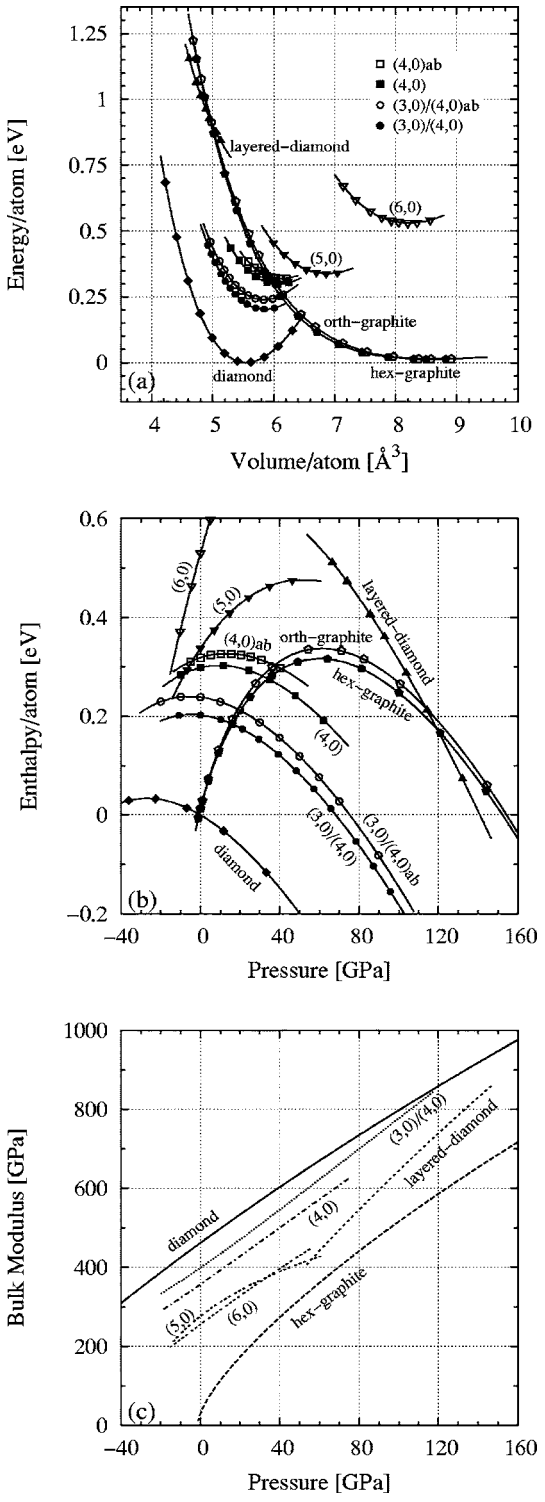

FIG. 3. Calculated (a) energy versus volume, (b) enthalpy versus pressure, and (c) bulk modulus versus pressure for the honeycomb structures and layered-diamond compared to graphite and diamond. In (a) and (b), the symbols represent calculated data points and the lines are numerical fits, and in (c) the bulk modulus is obtained from the second derivative of the numerical fit to the energy and the pressure from the first derivative of the same fit. In (b) the enthalpy is plotted relative to the enthalpy at the graphite to diamond transition and the line defined by $H=40a_0^3\times p$ has been subtracted for clarity.

TABLE I. Calculated zero pressure energy per atom, volume per atom, and bulk modulus values for several structures. Total energies are shown relative to the energy of cubic-diamond. Other available experimental and numerical values are also given for comparison.

Structure	E_0/atom [meV]	V_0/atom [Å^3] (calc.)	V_0/atom [Å^3] (other)	B_0 [GPa] (calc.)	B_0 [GPa] (other)
Cubic-diamond	0.0	5.55	5.67[a]	460	443[b]
Hex-graphite	12.0	8.61	8.80[c]	30	34[d]
Orth-graphite	12.8	8.64		40	
(3,0)/(4,0)	202.2	5.86		397	
(3,0)/(4,0)ab	238.6	5.84		411	
(4,0)	298.5	6.08		356	
(4,0)ab	318.6	6.13		361	
(5,0)	338.0	6.87		276	
(6,0)	530.3	8.21		255	252[e]

[a]Experiment, Reference 31.
[b]Experiment, Reference 32.
[c]Experiment, Reference 33.
[d]Experiment, Reference 34.
[e]Calculation, Reference 19.

Table I shows the values of zero pressure energy per atom, volume per atom, and bulk modulus for several studied structures, together with some experimental values. Experimentally the cohesive energy per atom of graphite is 25 meV larger than the cohesive energy of cubic-diamond.[35] On the other hand, in our calculation, graphite is metastable relative to cubic-diamond with an energy difference of 12 meV.

Previous DFT-LDA calculations[11–13] also show that the equilibrium energy of graphite is slightly higher than the equilibrium energy of diamond. This discrepancy is caused by the LDA's inaccurate description of the van der Waals interaction. Other approaches, like variational quantum Monte Carlo,[35,36] have been used to try to clarify this issue, but, because the energy difference is so small, the problem remains unresolved. In this work, however, this inaccuracy is not important for the relative stabilities of the high-pressure phases since, as the pressure is raised, the magnitude of the van der Waals interaction becomes small compared to the dominant electrostatic repulsion. Although some uncertainty on the transition pressures is present, in relative terms it is small in the high-pressure regime and the relative stabilities of the different high-pressure phases are well described. Another consequence of the underestimation of the van der Waals interaction is that at zero pressure, the energies of both hexagonal- and orthorhombic-graphite are essentially the same within the precision of our calculation. As the pressure increases, the enthalpy of orthorhombic-graphite is consistently higher than that of hexagonal-graphite for the range of pressures studied.

Figure 4 shows the density of states at zero pressure for all the metastable structures and at 120 GPa for graphite and layered-diamond. Hexagonal-graphite is a semi-metal, whereas cubic-diamond exhibits semiconducting behavior with a LDA energy gap of 4.2 eV (LDA tends to systematically underestimate the energy gap of semiconductors). The

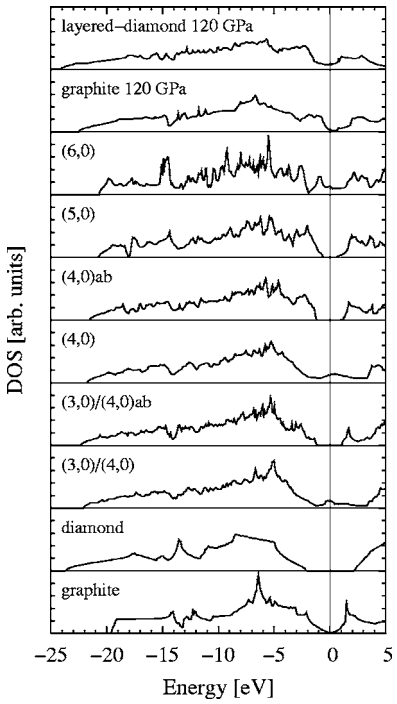

FIG. 4. Calculated electronic density of states for all the studied carbon structures. The top two plots show the density of states of hexagonal-graphite and layered-diamond at the transition pressure, 120 GPa, while all the other plots are at zero pressure. The Fermi level is at 0 eV.

(3,0)/(4,0), (4,0), and (6,0) honeycombs are metallic, and the (3,0)/(4,0)ab, (4,0)ab, and (5,0) are semiconducting with LDA energy gaps of 2.3, 2.3, and 1.6 eV, respectively. Because layered-diamond is not metastable at zero pressure, we compare the density of states of layered-diamond and hexagonal-graphite at the transition pressure of 120 GPa. Both layered-diamond and hexagonal-graphite at 120 GPa are metallic. For hexagonal-graphite, the DOS changes considerably from 0 to 120 GPa, with increased dispersion due to the reduction in volume. It is interesting to note that the very high bulk modulus systems (3,0)/(4,0), (4,0), and (6,0) are metallic.

The simulated x-ray-diffraction patterns of graphite at several pressures, cubic and hexagonal-diamond, (3,0)/(4,0)ab, and (3,0)/(4,0) honeycombs at 20 GPa are compared in Fig. 5 to the experimental x-ray-diffraction pattern of graphite powder under pressure adapted from Ref. 8. The simulated x-ray powder diffraction patterns are obtained by a simple model involving the squares of the structure factors. The calculated and experimental positions of the main graphite peaks for the different pressures agree quite well for pressures below the transition to the transparent phase. Above the transition pressure, the experimental diffraction peaks broaden significantly, and this broadening could be a result of buckling of the graphitic planes. No direct match is possible between the experimental peaks at high pressures and the simulated peaks for any of the five test structures. However, the strongest peaks for (3,0)/(4,0) and (3,0)/(4,0)ab honeycombs are located essentially in the region between 8 and 10.5 deg and 15 and 17 deg, which are

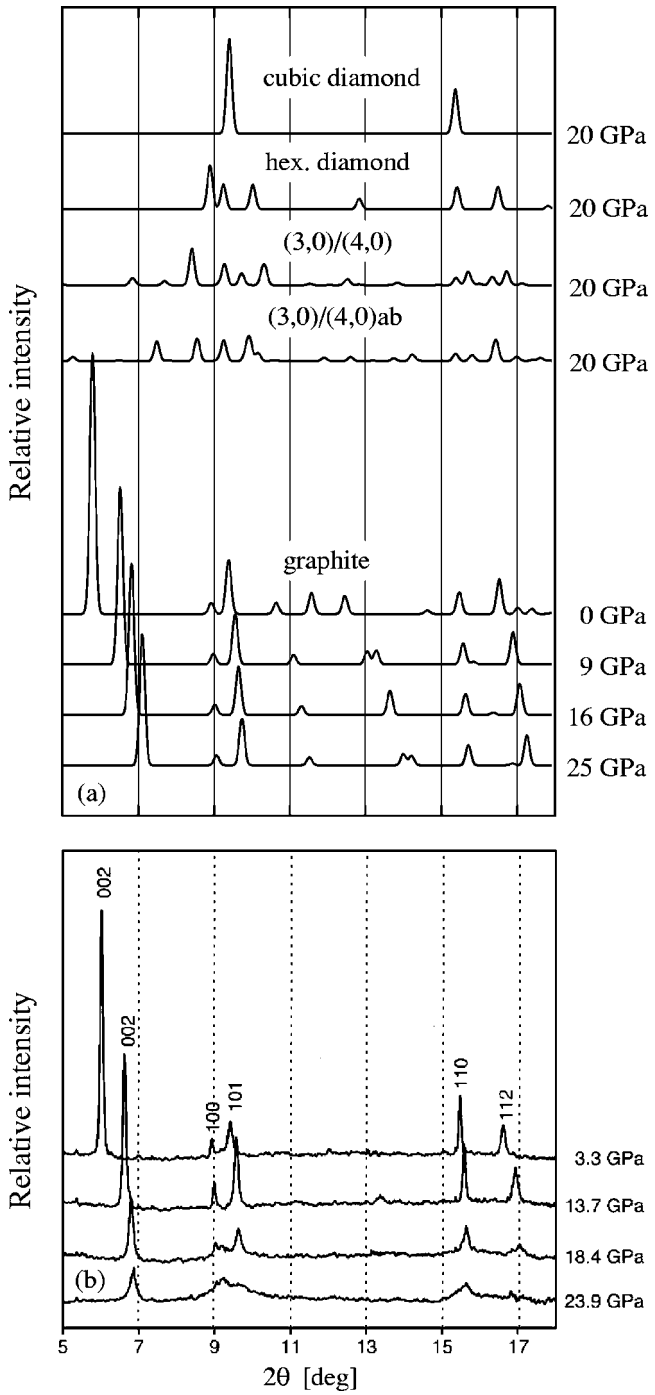

FIG. 5. Comparison between (a) calculated graphite, (3,0)/(4,0)ab, (3,0)/(4,0), hexagon and cubic-diamond, and (b) experimental graphite powder X-ray diffraction patterns adapted from Ref. 8 (x-ray energy of 37.45 KeV) for different pressures. The calculated patterns are based on a simple model, and therefore, only the position of the peaks should be trusted, not the amplitude.

exactly the extents of the broad experimental peaks. Also, the x-ray pattern might be consistent with a combination of several structures if one assumes that not all of the sample has undergone a transition or that the final phase is a combination of several phases.

V. CONCLUSIONS

In this work, the results of total energy calculations of several possible diamond-graphite hybrid structures of carbon were presented. One of these structures, layered-diamond, results from the direct buckling of hexagonal-graphite without plane sliding, and the pressure at which the enthalpies of both phases are the same—the transition pressure—is 120 GPa. Because of this very high pressure and the fact that the activation energy for plane sliding in graphite is very small, the experimental observation of this phase is very unlikely. Our calculations show that at pressures of 17, 20, 34, and 40 GPa graphite can transition to the honeycomb phases (3,0)/(4,0), (3,0)/(4,0)ab, (4,0), and (4,0)ab, respectively. As with the transitions to either cubic- or hexagonal-diamond the transitions to the honeycombs require sliding of the graphite planes, which transforms hexagonal-graphite into orthorhombic-graphite. Our calculations show that the energy difference between these two stackings of graphite is very small, and that the enthalpy of orthorhombic-graphite is always higher than that of hexagonal-graphite, which means that finite temperature is necessary for plane sliding. Experimentally, to transform graphite into diamond, temperatures above 1000 °C are necessary because of the large activation energy between the two phases. Although the activation barriers were not calculated in this work, it is plausible that the activation barriers for the transitions between graphite and the four honeycomb structures mentioned above are comparable to that of the transition between graphite and diamond because all the transitions considered involve the buckling of sp^2 hybridized orbitals into sp^3. Experimentally, a transparent phase is achieved by compression of graphite above 14 GPa at room temperature. Below 100 K, this phase is metastable relative to graphite. This means that there is a lower activation barrier than that for the transition to diamond, and the activation barrier for the reverse transition is very low. A detailed study of the activation barrier would clarify this issue, but this is left for future work. If we disregard the activation barrier issue, the most promising candidates for the transparent phase are the hybrid (3,0)/(4,0) and (3,0)/(4,0)ab structures, with transition pressures of 17 and 20 GPa, respectively. Both pressures are higher than the experimental pressure of 14 GPa. However, because of the inaccurate description of the van der Waals interaction within the LDA, there is a small uncertainty associated with the values of the transition pressures. The very low compressibility of these phases may explain the ring cracks observed in the diamond anvils.[8] Electronically, the (3,0)/(4,0)ab honeycomb was shown to be an insulator, which is in agreement with experimental evidence,[1,8] whereas (3,0)/(4,0) is a metal. The calculated x-ray-diffraction patterns of the possible candidates show similarities with the experimental pattern, but there is no clear agreement.

The activation energy discrepancy, the high-transition pressures for the honeycombs, and the x-ray mismatch suggest the possible existence of yet another structure. Other hybrid structures with higher ratios of (3,0) honeycombs relative to the wider (4,0)'s, would likely have lower equi-

librium energies, lower transition pressures, and lower volumes per atom. But as the density of (3,0) honeycombs is increased, the system gets closer to a hexagonal-diamond phase with some sp^2-sp^2 bonded stacking defects. In addition, the activation energy is likely to be very high. Therefore, hybrid $(3,0)/(4,0)$ structures with a high proportion of (3,0) honeycombs would probably be amorphous.

In conclusion, although we have studied likely candidates for the high-pressure, low-temperature transparent phase of carbon, its structural details remain unknown and further work is necessary.

ACKNOWLEDGMENTS

This work was supported by National Science Foundation Grant No. DMR04-39768 and by the Director, Office of Science, Office of Basic Energy Sciences, Division of Materials Sciences and Engineering, U.S. Department of Energy under Contract No. DE-AC03-76SF00098. Computational resources were provided by DOE at the National Energy Research Scientific Computing Center (NERSC), and NSF at the National Partnership for Advanced Computational Infrastructure (NPACI).

[1] F. P. Bundy, W. A. Bassett, M. S. Weathers, R. J. Hemley, H. K. Mao, and A. F. Goncharov, Carbon **34**, 141 (1996).
[2] R. Clarke and C. Uher, Adv. Phys. **33**, 469 (1984).
[3] R. B. Aust and H. G. Drickamer, Science **140**, 817 (1963).
[4] F. P. Bundy and J. S. Kasper, J. Chem. Phys. **46**, 3437 (1967).
[5] S. Scandolo, M. Bernasconi, G. L. Chiarotti, P. Focher, and E. Tosatti, Phys. Rev. Lett. **74**, 4015 (1995).
[6] K. J. Takano, H. Harashima, and M. Wakatsuki, Jpn. J. Appl. Phys., Part 2 **30**, L860 (1991).
[7] E. D. Miller, D. C. Nesting, and J. V. Badding, Chem. Mater. **9**, 18 (1997).
[8] W. L. Mao, H.-k. Mao, P. J. Eng, T. P. Trainor, M. Newville, C.-c. Kao, D. L. Heinz, J. Shu, Y. Meng, and R. J. Hemley, Science **302**, 425 (2003).
[9] Z. Wang, Y. Zhao, K. Tait, X. Liao, D. Schiferl, C. Zha, R. T. Downs, J. Qian, Y. Zhu, and T. Shen, Proc. Natl. Acad. Sci. U.S.A. **101**, 13699 (2004).
[10] A. Y. Liu and M. L. Cohen, Phys. Rev. B **45**, 4579 (1992).
[11] C. Mailhiot and A. K. McMahan, Phys. Rev. B **44**, 11578 (1991).
[12] S. Fahy, S. G. Louie, and M. L. Cohen, Phys. Rev. B **35**, 7623 (1987).
[13] S. Fahy, S. G. Louie, and M. L. Cohen, Phys. Rev. B **34**, 1191 (1986).
[14] R. Biswas, R. M. Martin, R. J. Needs, and O. H. Nielsen, Phys. Rev. B **30**, 3210 (1984).
[15] N. Hamada, S. I. Sawada, and A. Oshiyama, Phys. Rev. Lett. **68**, 1579 (1992).
[16] H. R. Karfunkel and T. Dressler, J. Am. Chem. Soc. **114**, 2285 (1992).
[17] A. T. Balaban, D. J. Klein, and C. A. Folden, Chem. Phys. Lett. **217**, 266 (1994).
[18] K. Umemoto, S. Saito, S. Berber, and D. Tománek, Phys. Rev. B **64**, 193409 (2001).
[19] N. Park and J. Ihm, Phys. Rev. B **62**, 7614 (2000).
[20] P. Hohenberg and W. Kohn, Phys. Rev. **136**, B864 (1964).
[21] W. Kohn and L. J. Sham, Phys. Rev. **140**, A1133 (1965).
[22] M. L. Cohen, Phys. Scr., T **T1**, 5 (1982).
[23] L. Kleinman and D. M. Bylander, Phys. Rev. Lett. **48**, 1425 (1982).
[24] J. L. Martins, N. Troullier, and S.-H. Wei, Phys. Rev. B **43**, 2213 (1991).
[25] The *k*-point mesh for diamond was $6\times6\times6$ and even denser grids were used for other semiconductor systems; the *k*-point mesh for graphite was $12\times12\times8$ and even denser grids were used for other metallic systems. To calculate the DOS the *k*-point meshes were double in all three directions.
[26] J. P. Perdew and A. Zunger, Phys. Rev. B **23**, 5048 (1981).
[27] D. M. Ceperley and B. J. Alder, Phys. Rev. Lett. **45**, 566 (1980).
[28] B. G. Pfrommer, M. Côté, S. G. Louie, and M. L. Cohen, J. Comput. Phys. **131**, 233 (1997).
[29] P. E. Blöchl, O. Jepsen, and O. K. Andersen, Phys. Rev. B **49**, 16223 (1994).
[30] D. W. Brenner, O. A. Shenderova, J. A. Harrison, S. J. Stuart, B. Ni, and S. B. Sinnott, J. Phys.: Condens. Matter **14**, 783 (2002).
[31] C. Kittel, *Introduction to Solid State Physics*, 7th ed. (Wiley, New York, 1996).
[32] H. J. McSkimin and J. P. Andreactch, J. Appl. Phys. **43**, 985 (1972).
[33] J. Donohue, *The Structure of Elements* (Wiley, New York, 1974).
[34] P. Bridgeman, Proc. Am. Acad. Arts Sci. **76**, 9 (1945).
[35] S. Fahy, X. W. Wang, and S. G. Louie, Phys. Rev. B **42**, 3503 (1990).
[36] D. Prendergast, D. Bevan, and S. Fahy, Phys. Rev. B **66**, 155104 (2002).